Research Square

Preprints are preliminary reports that have not undergone peer review.
They should not be considered conclusive, used to inform clinical practice,
or referenced by the media as validated information.

Sex-specific trajectories of adolescent brain maturation and sensorimotor gating after maternal influenza infection in mice

Christos Pantelis

cpant@unimelb.edu.au

The University of Melbourne https://orcid.org/0000-0002-9565-0238

Danli Peng

Antonia Merritt

KH Christopher Choy

https://orcid.org/0000-0002-4650-2220

Stella Liong

RMIT University, Australia

Robert Brkljača

Cassandra Wannan

The University of Melbourne https://orcid.org/0000-0003-1317-4635

Ulysse Thivisol

David K. Wright

Monash University

Arthur Christopoulos

Monash University https://orcid.org/0000-0003-4442-3294

Jess Nithianantharajah

University of Melbourne https://orcid.org/0000-0002-3501-1143

Stavros Selemidis

Warda Syeda

University of Melbourne https://orcid.org/0000-0001-6294-622X

Article

Keywords:

Posted Date: August 13th, 2026

DOI: https://doi.org/10.21203/rs.3.rs-10546527/v1

License: This work is licensed under a Creative Commons Attribution 4.0 International License.
Read Full License

Additional Declarations: The authors have declared there is **NO** conflict of interest to disclose

Abstract

Maternal infection during pregnancy is increasingly recognised as a risk factor for neurodevelopmental disorders, yet how a clinically relevant viral insult reshapes brain maturation remains poorly defined. Here, we used a live influenza A virus model of maternal immune activation (MIA) to examine whether prenatal infection alters offspring brain development across adolescence. Pregnant mice were infected at embryonic day 12, and offspring underwent longitudinal high-field MRI at 5, 8, 11 and 14 weeks, followed by prepulse inhibition (PPI) testing as a measure of sensorimotor gating. Maternal influenza exposure produced sex- and age-dependent alterations in brain maturation. Atlas-based volumetry identified FDR-corrected sex- and age-dependent treatment-related effects in the hippocampal CA1 region, while tensor-based morphometry revealed dynamic structural changes across sensory cortices, insula, hippocampus and thalamus. Network analyses further showed disrupted inter-regional structural coordination, particularly in males during early–mid adolescence. Despite partial normalisation of network architecture by late adolescence, influenza-exposed offspring displayed impaired PPI. Partial least squares regression linked these behavioural deficits to altered developmental trajectories in somatosensory cortex, medulla and pons. These findings show that maternal influenza infection does not simply produce static brain abnormalities but alters the trajectory and coordination of adolescent brain maturation in a sex-, region- and circuit-specific manner with long-term behavioural consequences. This work identifies developmental windows and neural systems that may guide future strategies to prevent or reverse infection-associated neurodevelopmental vulnerability.

Introduction

Neurodevelopmental disorders, including autism spectrum disorder (ASD) and schizophrenia spectrum disorders (SSD), likely arise from altered developmental trajectories beginning prenatally, when the foetal brain is sensitive to genetic, immune and environmental cues[1,2]. Although these disorders are highly heritable[3], genetics alone cannot account for their onset, timing or clinical heterogeneity[4]. The prenatal period represents a critical window, when factors like maternal infection and inflammation may act to shape later neuropsychiatric trajectories and outcomes[5–7], including influenza virus-related immune activation increasing the risk for schizophrenia-related outcomes[8]. However, the biological events linking a transient maternal immune challenge to long-term changes in offspring brain maturation remain difficult to resolve in humans. Preclinical models therefore provide an essential platform to identify vulnerable developmental windows, circuits and behaviours that are most vulnerable to disruption from early insults, without the ethical concern as in human study[9,10].

Maternal immune activation (MIA) provides a powerful experimental framework to model how infection or inflammation during pregnancy alters offspring brain development[11]. Traditionally, MIA has been induced using immune mimetics such as polyinosinic:polycytidylic acid [poly(I:C)], lipopolysaccharide (LPS), or inflammatory cytokines such as interleukin-6[12,13]. These approaches establish that maternal immune responses can disrupt neurodevelopment without direct foetal infection[12,13]. However, immune

mimetics capture only part of the biology of maternal infection. In contrast, live influenza A virus (IAV) engages viral sensing pathways, antiviral immunity, cytokine induction, antibody responses and systemic maternal pathology, including inflammatory and vascular dysfunction[14,15]. This distinction is critical, because clinically relevant maternal viral infection is not a single immune signal, but a coordinated and dynamic host response. Live-virus MIA models may therefore better represent how maternal infection reshapes foetal and postnatal brain development[15].

Longitudinal neuroimaging can reveal how prenatal immune challenge alters trajectories of brain maturation[16,17], where MIA effects may emerge, evolve or partially normalise across adolescence[16]. Structural MRI enables repeated, non-invasive assessment of regional brain growth, and tensor-based morphometry (TBM) can quantify both anatomically defined and spatially localised brain changes. The hippocampus is of particular interest because of its role in learning, memory and spatial navigation, has well-established involvement in schizophrenia and related disorders[18–21], and is implicated in MIA-associated brain pathology[22,23]. Longitudinal analysis of its subfields may therefore identify specific time-variant disruptions rather than a whole-region measure.

To understand the mechanistic bridge between prenatal immune challenge and later-emerging abnormalities, prepulse inhibition (PPI) provides a behavioural readout of sensorimotor gating, which is disrupted in schizophrenia and other neurodevelopmental disorders[24]. PPI deficits occur in both human cohorts with schizophrenia and pre-clinical MIA models, including our previous work showing impaired PPI in IAV-infected dams[24–26]. However, most studies have treated PPI and other behaviours as endpoint phenotypes, with limited insight into the developmental brain trajectories that give rise to impairment. Linking longitudinal MRI to PPI can identify the regions and maturational patterns associated with impaired sensorimotor gating after prenatal viral immune challenge.

Here, we leveraged a clinically relevant live IAV model of MIA to determine how prenatal viral immune challenge alters offspring brain maturation across adolescence. Pregnant mice were infected at embryonic day 12, and offspring underwent longitudinal high-field MRI at 5, 8, 11 and 14 weeks, followed by PPI testing in early adulthood. We combined atlas-based segmentation, longitudinal tensor-based morphometry, inter-regional structural correlation network analysis and partial least squares (PLS) regression to define how maternal IAV exposure affects regional brain growth, local morphometry, network organisation and structure–behaviour relationships. We focused particularly on sex-specific effects, given the known sex bias in neurodevelopmental vulnerability following prenatal immune challenge. This design allows us to move beyond static endpoint measures to test whether maternal influenza disrupts the tempo of adolescent brain maturation, creating circuit-level vulnerabilities that persist as impaired sensorimotor gating.

Materials and Methods

Animals and maternal influenza infection

All animal experiments were conducted at the Baker Institute Animal Facility (PAC) and Imaging Facility in Melbourne, Australia, in accordance with the National Health and Medical Research Council (NHMRC) of Australia guidelines for animal experimentation and with approval from Animal Ethics Committee of the Monash Institute of Pharmaceutical Sciences (AEC# 29379). C57BL/6J breeding mice were obtained from the Monash Animal Research Platform and acclimatised for 7 days before time-mating. Females were paired with males at a 1:1 ratio. Mice were housed under a 12 h light/dark cycle at 22°C and 40–60% humidity, with standard chow and water available *ad libitum*. Plugged dams were housed individually in micro-isolator cages.

Mouse-adapted HKx31 influenza A virus (IAV; H3N2) was propagated in 10-day-old embryonated chicken eggs. Viral titres were quantified by plaque assay using Madin-Darby Canine Kidney cells, as previously described[27], and virus stocks were stored at −80°C.

At embryonic day 12 (E12) of pregnancy, dams were anesthetised with isoflurane and randomly allocated to either the IAV group or phosphate buffered saline (PBS) control group in a balanced 1:1 design (n = 4 dams per group). Dams received intranasal inoculation with either 35µl of 10^3 PFU IAV or PBS as previously described[27]. This dose and gestational timing were selected because they induce MIA while minimising offspring lethality[15]. Maternal body weight was recorded daily from E12 to E16, after which dams were left undisturbed until delivery at approximately E19–E20. Offspring were weaned at 3–3.5 weeks of age and group-housed by sex, with 2–5 mice per cage, under reverse light-cycle conditions. Following completion of behavioural testing, mice were rested for 2–3 days and then euthanised by cervical dislocation.

Magnetic resonance imaging (MRI) acquisition

Longitudinal *in vivo* MRI was performed at 5 (early adolescence), 8 (mid adolescence), 11 (late adolescence) and 14 (early adulthood) weeks of age using a 9.4T small-animal MRI scanner with a mouse room-temperature surface coil (Bruker, USA). Immediately before scanning, mice were anaesthetised using 5% isoflurane in 0.5 – 1L/min in medical grade oxygen and positioned in an MRI compatible animal holder with anaesthesia maintained via a nose cone. Isoflurane concentration was adjusted throughout scanning to maintain stable anaesthesia. Respiratory rate was monitored via a pressure sensor and maintained within 45 – 70 breaths per minute. Body temperature was monitored using a rectal probe and maintained at 37°C with a purpose-built circulating hot-water warming system.

Multi-echo gradient echo (GRE) scans were acquired with the following parameters: echo time (TE) 2.1 ms; inter-echo spacing (dTE) 3.1 ms, 12 echoes; Repetition Time (TR) 66 ms; matrix size 174x144x80; Field of View (FOV) 17.4x14.4x8 mm^3; voxel size 100 x 100 x 100 μm^3; and four repetitions.

Figure 1 here

Atlas-based volumetric analysis

Multi-echo T2*-weighted images were corrected for bias-field inhomogeneity using N4ITK and averaged across echoes to improve anatomical contrast[28]. Brain extraction was performed using Brain Extraction Net, which was first fine-tuned using existing skull-stripped mouse MRI data and then applied to the full dataset[29]. The ANTs software toolkit[28] was used for volumetric analysis to create group-specific templates for each treatment and sex at each time point, which were then merged to form a comprehensive study template. This study template underwent nonlinear registration to the Allen Mouse Brain CCFv3 using AIDAmri based on NiftyReg, enabling us to accurately segment brain areas (including hippocampal subfields)[28,30,31]. Nonlinear registrations were applied from individual subject images to the study template for precise region of interest delineation. Manual adjustments were made where necessary on the study template mask. Finally, each region volume was determined by counting the number of voxels it contained.

A linear mixed-effects model was employed in MATLAB using the 'fitlme' function to investigate the interaction of treatment group, sex, and age on brain region volumes longitudinally. Random effects included intercepts for individual animals and fixed effects for treatment, sex, and age, with age modelled using linear, quadratic and cubic terms. Model residuals were tested for normality using a Q-Q plot and histogram overlaying a standard normal distribution, in addition to using the Lilliefors test for normality corroboration. This model accounted for the fixed effects of treatment group, sex, and age, as well as their interactions up to the cubic term for age, thereby effectively handling longitudinal repeated measures data. P-values from the atlas-based volumetric analysis were corrected for multiple comparisons using the Benjamini–Hochberg false discovery rate (FDR) procedure.

Tensor-Based Morphometry (TBM)

Tensor-based morphometry was used to assess localised differences in brain morphology across development. Aligned raw data from each individual were initially registered to a Minimum Deformation Template (MDT) created from PBS images. Non-linear registrations of individuals to MDT were performed to obtain the absolute Jacobian determinants, ensuring local anatomical variations were captured and facilitating exact comparison of morphological differences across individuals. Following registration, deformation fields from each individual data to the MDT were analysed by the log Jacobian determinant, providing a voxel-wise representation of local volume changes rate (expansion or contraction) relative to the MDT.

Statistical analysis of TBM data was completed using linear mixed effects model — voxel-wise models were used to examine treatment group, sex, and age effects while accounting for longitudinal data structure. Fixed effects included treatment group, sex, and age, together with their interactions. Random effects included individual intercepts. A permutation (5000 times random shuffling of treatment and sex labels) approach for correction in multiple comparisons was used for data analysis. At each permutation, clusters of voxels with statistical significance greater than $|t| > 3$ were identified, and the maximum sum of the t-statistic over voxels in each cluster was taken. Significant threshold p-values were thus identified using the resulting distribution of maximum sums under the null.

Graph theoretical analysis of inter-regional structural correlations

Graph theoretical analyses were used to examine whether maternal IAV exposure altered the coordination of regional brain growth across development. For each sex and treatment group, Spearman's rank correlation matrices were generated from longitudinal changes in regional brain volumes. Correlations were calculated between all pairs of brain regions using percentage volume change across consecutive imaging intervals: 5–8 weeks, 8–11 weeks, and 11–14 weeks. This approach allowed us to assess whether regional brain maturation occurred in a coordinated or disrupted manner across development. Correlation matrices were thresholded at Spearman's $\rho = 0.625$ to retain robust inter-regional associations while reducing the influence of weak or potentially spurious correlations. Network organisation was then assessed using graph theoretical metrics, including Jaccard similarity index, characteristic path length, assortativity, closeness centrality and transitivity. Jaccard similarity was used to quantify the similarity of network architecture between treatment groups, characteristic path length to assess global network integration, assortativity to determine whether nodes preferentially connected with other nodes of similar degree, closeness centrality to estimate nodal communication efficiency, and transitivity to assess local clustering. Community structure was examined using the Louvain method.

Prepulse inhibition (PPI) testing

Prepulse inhibition test was conducted 3-4 days after the final MRI scan at 14 weeks of age. Mice underwent a mock PPI session for habituation, followed by the test session 24 h later, as described previously[15,25]. Two-way ANOVA was conducted to examine main effects of treatment (PBS vs. IAV) and sex, and their interactions, followed by post hoc analyses where appropriate.

Structure–behaviour modelling

Partial least squares (PLS) regression was used to explore correlations between structural brain developmental trajectory parameters (intercept, 1^{st}, 2^{nd}, 3^{rd} order coefficients) and behavioural performance in the PPI test. All brain region data (X matrix; per-subject trajectory parameters for each region of interest: intercept, linear, quadratic terms) matched with PPI values – Y matrix was examined through 10 components (selected by cross-validation) to identify key patterns linking brain structure to behaviour. Singular Value Decomposition (SVD) of X and Y scores quantified the strength of correlation, where permutations (10,000) were carried out to calculate a p value comparing actual association with random permutations. To estimate the variability of X loadings, bootstrap resampling was performed (1000) at the significance of 0.05, identifying brain regions significantly associated with PPI. A linear regression model incorporating both main effects and interactions between sex and MIA (PLS component ~ Sex * MIA) was employed to identify how sex or MIA effects were determined from the latent variables of the PLS analysis to better understand the biological meanings of the PLS components. Permutation testing (1,000) was performed to validate the significance of these associations. Univariate linear regression models were then established to investigate the relationships

between the significant trajectory parameters of brain regions identified through longitudinal MRI analysis and PPI performance.

Results

All offspring included in the study completed the longitudinal MRI protocol and subsequent PPI testing. The final cohort comprised 27 mice across four groups: PBS females (n = 7), PBS males (n = 7), IAV females (n = 7), and IAV males (n = 6). Offspring underwent MRI at 5, 8, 11 and 14 weeks of age, followed by PPI testing at 14.5 weeks. This design enabled longitudinal assessment of regional brain growth, local morphometric change, inter-regional structural coordination and structure–behaviour relationships following maternal IAV exposure.

Maternal IAV exposure alters sex-specific hippocampal CA1 development

Atlas-based volumetric analysis was used to examine whether maternal IAV exposure altered regional brain growth trajectories across adolescence. Linear mixed-effects modelling identified Field CA1 as the only atlas region showing treatment-related sex- and age-dependent developmental effects after FDR correction. The treatment × sex × age term in CA1 was significant before and after FDR correction (raw $p = 0.000269$; FDR-adjusted $p = 0.0242$; adjusted $R^2 = 0.90$; Fig. 2; Plot with individual datapoints is in Supplementary Materials (Fig. 1)). This indicates that maternal IAV exposure altered CA1 maturation in a sex-dependent manner across development. Visualisation of individual and group-level trajectories showed divergent CA1 growth patterns between male and female offspring following maternal IAV exposure. Although additional regions, including the ventricles, cerebral cortex, hippocampal-associated structures, cortical subplate, brain nuclei, brainstem and cerebellum, showed nominal evidence of MIA-related developmental interaction effects, these did not survive FDR correction and are reported in the Supplementary Materials (Fig. 2–7).

* Fig. 2 here *

Longitudinal TBM reveals distributed sex-specific disruption of brain maturation

To identify localised morphometric changes beyond predefined atlas regions, we performed longitudinal tensor-based morphometry across the adolescent imaging period. This analysis identified significant MIA × age × sex interactions in multiple brain regions after cluster-based correction (Fig. 3, and other interactions listed in Supplementary Materials (Fig. 8–10)), indicating that maternal IAV exposure altered local brain maturation in a sex- and age-dependent manner. Significant clusters were detected across cortical, sensory, hippocampal and thalamic regions, including the agranular insular, orbital, motor, olfactory, gustatory, auditory and visual cortices, as well as CA1, CA3, ventral striatum and thalamus. The largest interaction effects were observed in primary visual areas. Male offspring showed predominant

effects across cortical regions, including agranular insular, orbital, motor and visual areas, whereas female offspring showed more prominent alterations in inner brain structures, particularly the thalamus and hippocampal CA3 regions. Together, these findings indicate that maternal IAV exposure does not produce a uniform structural phenotype but instead disrupts local brain maturation in a regionally and sexually divergent manner.

* Fig. 3 here *

Maternal IAV disrupts adolescent structural network maturation in a sex-dependent manner.

We next examined whether maternal IAV exposure altered the coordinated maturation of brain regions across adolescence. Graph theoretical analysis of inter-regional structural correlation networks revealed marked network reorganisation in IAV-exposed male offspring compared with PBS males (Fig. 4). This was reflected by a significantly reduced Jaccard similarity index (0.36, p = 0.0339), indicating substantial divergence in network architecture between treatment groups. IAV-exposed males also showed increased closeness centrality compared with PBS males (30% increase, p = 0.0321), consistent with altered patterns of inter-regional structural coordination. Louvain community detection further supported modular reconfiguration in IAV-exposed males relative to controls. (see Supplementary Materials Fig. 12).

To determine when these network changes were most pronounced, we examined regional volume-change correlations across consecutive developmental intervals (see Supplementary Materials (Fig. 11–14)). From 5–8 weeks (early-mid adolescence), females in the IAV group showed a lower Jaccard similarity index (0.36, *p = 0.034*), indicating network reorganisation during early development. In IAV males over the same interval, characteristic path length increased by 4% (*p = 0.040*) for positive-correlation networks, while assortativity in the negative-correlation networks dropped sharply (~ 50-fold; *p = 0.0083*; see Supplementary). Between 8 and 11 weeks, IAV-exposed males also showed reduced transitivity (11% decrease, p = 0.040), together with increased positive correlations between hippocampal and extra-hippocampal regions (p = 0.03; Supplementary Materials). No significant network differences were detected between 11 and 14 weeks. Together, these findings localise the most pronounced network instability is apparent in early–mid adolescence, with earlier modular reorganisation in females and reduced integration in males. In contrast, by late adolescence the network architecture has normalised, and no sex differences were apparent.

* Fig. 4 here *

Maternal IAV impairs sensorimotor gating and links altered brain maturation to behaviour.

We next examined whether altered brain developmental trajectories following maternal IAV exposure were associated with behavioural dysfunction. Consistent with our previous findings[15], offspring from IAV-infected dams showed impaired prepulse inhibition at 14.5 weeks compared with PBS controls, indicating reduced sensorimotor gating (main effect of treatment: F(1,28) = 5.261, p = 0.030; Fig. 5A). No

significant main effects of sex or treatment × sex interaction were detected, although IAV-exposed males showed greater variability in PPI performance.

* Fig. 5 here *

To determine whether this behavioural phenotype was related to altered brain maturation, we used PLS regression to link regional developmental trajectory parameters with PPI performance. This analysis identified a significant association between longitudinal brain structure and sensorimotor gating ($p = 0.01$). The first PLS component explained 54% of the variance and was significantly associated with maternal IAV exposure ($p = 0.005$), while the second component explained 9% of the variance and was associated with sex ($p = 0.007$; Fig. 5B,C).

Bootstrap sampling identified brain regions whose trajectory parameters within Component 1 were significant. In the somatosensory areas, the cubic term (bootstrap ratio = 5.0822, $p = 3.7e-07$) and the linear term (bootstrap ratio = -7.1356, $p = 9.6e-13$) were significant. The medulla showed a positive linear term (bootstrap ratio = 4.0644, $p = 4.8e-05$) together with a negative cubic term (bootstrap ratio = -3.1816, $p = 0.001$). In the brainstem, the pons exhibited a positive linear term (bootstrap ratio = 2.9316, $p = 0.003$) alongside a negative cubic term (bootstrap ratio = -2.3132, $p = 0.02$), suggesting non-linear pattern changes associated with MIA.

To further probe region- and trajectory-shape–specific (polynomial terms) relationships in these significant regions, linear models linking each trajectory parameter to PPI were fitted, allowing for sex and MIA main effects and interactions. The Bayesian Information Criterion (BIC) was used to select the best model per parameter (see Fig. 5D). In the somatosensory areas, and mirroring findings in the PLS loadings, the linear and cubic term associations with PPI were group dependent, with a more negative slope for the linear term in MIA relative to PBS (Shape×MIA, $p = 0.014$, adjusted $R^2 = 0.544$), and the cubic term showed a positive MIA-specific modulation (Shape×MIA, $p = 0.036$, adjusted $R^2 = 0.492$). In the medulla, we likewise observed a positive slope in the linear term ($p = 0.036$, adjusted $R^2 = 0.374$) with only the MIA main effect. For the cubic term, the negative slope was specific to MIA (Shape×MIA, $p = 0.0378$, adjusted $R^2 = 0.464$). In the pons, both the linear and cubic terms were significantly linearly associated with PPI but without any interaction – positive linear ($p = 0.003$, adjusted $R^2 = 0.271$) and negative cubic ($p = 0.0025$, adjusted $R^2 = 0.284$). As shown in the Fig. 5D, the MIA animals have significantly smaller linear term ($|t| = 3.8$, $p = 0.001$), and larger cubic term ($|t| = 3.8$, $p = 0.001$). Taken together, these linear modelling results converge with the PLS findings, showing that MIA-related PPI deficits are most tightly coupled to developmental trajectories in the somatosensory cortex and brainstem, with linear changes complemented by higher-order nonlinear components.

Discussion

In this study, we show that maternal influenza infection reshapes offspring brain maturation across adolescence rather than producing a single neuroanatomical phenotype. Using a clinically relevant live IAV model of maternal immune activation, combined with longitudinal high-field MRI, structural network

analysis and behavioural testing, we found that prenatal viral immune challenge altered brain development in a sex-, age- and region-specific manner. Atlas-based volumetry identified the hippocampal CA1 region as a key locus of altered maturation, while longitudinal TBM revealed broader changes across sensory cortices, insula, hippocampus and thalamus. Structural correlation analyses further showed that maternal IAV disrupted the coordinated maturation of inter-regional brain networks, particularly in males during early–mid adolescence. Importantly, these developmental changes were behaviourally relevant: IAV-exposed offspring showed impaired prepulse inhibition, and structure–behaviour modelling linked this deficit to altered maturation of somatosensory and brainstem circuits. Together, these findings suggest that prenatal viral infection can shift the tempo and coordination of adolescent brain development, creating transient windows of structural instability with lasting consequences for sensorimotor gating.

The hippocampal findings provide an important anchor for this developmental interpretation. Atlas-based volumetry identified CA1 as the only region showing treatment-related sex- and age-dependent developmental effects after FDR correction, while longitudinal TBM further supported localised effects in CA1 and CA3. These findings suggest that maternal IAV exposure alters hippocampal maturation in a subfield-specific and sex-dependent manner, rather than producing uniform hippocampal volume loss. This is biologically plausible given that hippocampal subfields follow distinct developmental programs[32], with CA1 and CA3 emerging during mid-gestation (approximately E14-E16) and continuing to mature across postnatal life. The timing of maternal IAV exposure at E12 may therefore intersect with a critical period of hippocampal specification and circuit formation. Importantly, hippocampal abnormalities are among the most consistent structural findings in schizophrenia-spectrum disorders, including first-episode psychosis and established illness. Our findings extend this literature by showing that prenatal viral immune challenge can alter the trajectory of hippocampal maturation across adolescence, with male offspring showing particular vulnerability in CA1 development.

Longitudinal TBM extended the atlas-based findings by revealing distributed, spatially localised effects of maternal IAV exposure across the adolescent brain, and has been widely used in prior studies[16,33,34]. Rather than producing a single regional abnormality, prenatal viral immune challenge altered local morphometric trajectories across sensory cortices, insula, hippocampus, ventral striatum and thalamus. These effects were strongly sex-dependent: male offspring showed predominant alterations across cortical regions (insular, orbital, motor and visual areas), whereas females showed changes in inner brain structures (particularly thalamus and hippocampal CA3). This regional divergence suggests that maternal IAV exposure perturbs distinct developmental programs in males and females, consistent with evidence that prenatal immune challenge can shape brain development in a sex-specific manner[35]. Although some trajectories appeared to partially normalise over time, particularly in females, we interpret this cautiously as evidence of divergent developmental responses rather than definitive resilience. Whether these patterns reflect compensatory recovery, altered developmental timing or distinct cellular adaptations will require further mechanistic validation. The prominence of sensory cortical and thalamic changes is notable given the role of these systems in sensory processing, salience detection and

sensorimotor integration, processes frequently disrupted in neurodevelopmental and schizophrenia-spectrum disorders[36,37]. These findings are consistent with previous live-IAV MIA work showing brain-region-specific alterations in offspring gene-expression trajectories across development, involving pathways for neuroinflammation, complement and microglial biology[15]. Thus, the TBM findings broaden the impact of maternal IAV beyond the hippocampus and support the view that prenatal viral immune challenge disrupts coordinated maturation across distributed brain systems.

Network analyses provided further evidence that maternal IAV exposure alters the coordination of adolescent brain maturation. During normal development, brain organisation shifts from more locally clustered patterns toward more distributed and integrated networks[38,39]. Here, IAV-exposed males showed marked reorganisation of inter-regional structural correlation networks during early–mid adolescence. These findings suggest that maternal viral immune challenge disrupts not only the growth of individual brain regions, but also the coordinated maturation of relationships between regions, reinforcing observations of circuit and network dysregulation in neurodevelopmental disorders[20,40–43]. The timing of these effects is also highlighted, with network disruption most evident between 5 and 11 weeks, corresponding to an adolescent window of active brain refinement and increasing network efficiency[38,44–46]. Females showed earlier network reorganisation, while males showed more persistent disruption, consistent with known sex differences in immune vulnerability[47]. No significant network differences were detected between 11 and 14 weeks, suggesting partial normalisation of structural network architecture by late adolescence. However, this apparent normalisation should be interpreted cautiously, as behavioural deficits in PPI persisted. Thus, even if some structural network measures recover, early disruption in the timing and coordination of brain maturation may leave lasting functional consequences.

The behavioural findings indicate that these altered developmental trajectories have functional consequences. Both human and preclinical MIA offspring exposed to maternal IAV showed impaired PPI in early adulthood, reflecting disrupted sensorimotor gating [15,24,48,49]. Importantly, our structure–behaviour analysis extended these findings by linking impaired PPI to altered developmental trajectories in the somatosensory cortex, medulla and pons. This is significant because PPI is often discussed in relation to cortico-striatal and limbic circuitry, yet the startle response and its modulation also depend on brainstem sensorimotor pathways where auditory and sensory information converge to regulate motor output[50–53]. Our findings therefore suggest that maternal IAV exposure disrupts a broader sensorimotor gating circuit, involving both cortical sensory-processing regions and brainstem structures that directly participate in startle regulation. By linking PPI deficits to longitudinal trajectory parameters, these data support the notion that behavioural dysfunction emerges from altered maturational timing across adolescence. Thus, maternal viral immune challenge may leave a lasting behavioural alteration by shifting the developmental path of cortical and brainstem circuits that support sensorimotor gating.

These findings have relevance for understanding how prenatal infection may contribute to neurodevelopmental vulnerability in humans. Hippocampal abnormalities are among the most

consistent structural findings in schizophrenia-spectrum disorders, with reduced hippocampal volumes reported across first-episode psychosis, chronic schizophrenia and ultra-high-risk populations[18–20,54–56]. More recent work has further implicated hippocampal subfields, including CA1, in the transition from risk states to psychosis, with altered hippocampal metabolism and structure proposed to reflect early circuit dysfunction[57–59]. Our findings extend this clinical literature by showing that prenatal viral immune challenge can alter the developmental trajectory of hippocampal maturation before overt adult behavioural dysfunction is assessed. Rather than identifying a hippocampal abnormality at a single endpoint, our longitudinal design shows that maternal IAV exposure changes how hippocampal subfields develop across adolescence. This provides a preclinical framework for understanding how prenatal infection may shift the timing, tempo and circuit integration of hippocampal maturation in ways relevant to later neuropsychiatric risk.

A major strength of this study is the use of live IAV to induce maternal immune activation. Much of the MIA literature has relied on immune mimetics such as poly(I:C), LPS or cytokine administration, approaches that have defined how maternal inflammation can alter offspring neurodevelopment[11–13]. However, live viral infection engages a broader and more dynamic host response, including viral sensing, antiviral immunity, cytokine induction, antibody generation and systemic maternal pathology[14,15,27,60]. In the context of pregnancy, IAV also produces maternal inflammatory and vascular dysfunction, providing a clinically relevant model of the physiological stress imposed by respiratory viral infection[15,27]. Our findings therefore extend previous longitudinal MIA imaging studies using immune mimetics by demonstrating that a live maternal viral infection is sufficient to alter adolescent brain maturation trajectories, disrupt structural network organisation and impair sensorimotor gating[16,33]. This distinction is important because human prenatal infection risk is unlikely to be driven by a single inflammatory signal, but by the integrated maternal response to infection across immune, vascular and developmental systems.

Several limitations should be considered when interpreting these findings. First, although longitudinal MRI allowed repeated within-subject assessment of brain maturation, the study did not include histological, molecular or cellular validation of the regions identified through imaging. As a result, we cannot determine whether the observed structural trajectories reflect altered neurogenesis, synaptic pruning, gliosis, myelination, vascular remodelling or other cellular processes. Second, the cohort size was modest, particularly for sex-stratified network analyses. The repeated-measures design increased sensitivity to developmental trajectories, but larger cohorts will be required to validate the network findings and resolve more localised sex-specific effects. Third, PPI was assessed at a single adult time point. Repeated behavioural testing across adolescence would help determine whether sensorimotor gating deficits emerge in parallel with the structural changes identified by MRI, or whether they arise after earlier maturational disruption. Finally, this study focused on structural MRI and PPI; future studies incorporating diffusion imaging, functional measures, transcriptomics, immunophenotyping and broader behavioural assays will be needed to define the cellular mechanisms linking maternal IAV exposure to altered brain maturation and behavioural outcome.

In conclusion, we demonstrate that maternal influenza infection can alter the trajectory and coordination of offspring brain maturation across adolescence. Using a clinically relevant live IAV model, longitudinal high-field MRI, structural network analysis and behavioural testing, we identified evidence that prenatal viral immune challenge disrupts hippocampal, sensory cortical, thalamic and brainstem developmental programs in a sex- and age-dependent manner. Importantly, these changes were not limited to static anatomical differences but reflected altered maturational trajectories and network organisation that were linked to impaired sensorimotor gating. These findings position maternal viral infection as a developmental perturbation capable of shifting the timing, tempo and circuit organisation of the adolescent brain. More broadly, they provide a framework for understanding how prenatal infection may create windows of neurodevelopmental vulnerability relevant to schizophrenia-spectrum and related neurodevelopmental disorders.

Declarations

Declaration of interest

The authors declare no competing interests.

Acknowledgements

This research was funded by a National Health and Medical Research Council (NHMRC) Program Grant (A.C., C.P.; ID: 1150083). C.P. was supported by a NHMRC L3 Investigator Grant (ID: 1196508). D.K.W. is supported by a FightMND Mid-Career Research Fellowship (MCR-202503-01826_Wright). J.N. was supported by a One in Five Foundation McIver Research Fellowship. The authors acknowledge the facilities and scientific and technical assistance of the National Imaging Facility (NIF), a National Collaborative Research Infrastructure Strategy (NCRIS) capability at Monash Biomedical Imaging (MBI), a Technology Research Platform at Monash University.

Code availability

Code is available upon request.

References

1. Álvarez-Mejía, D., Rodas, J. A. & Leon-Rojas, J. E. From womb to mind: prenatal epigenetic influences on mental health disorders. *Int. J. Mol. Sci.* 26, 6096 (2025).
2. Ji-Xu, A. & Vincent, A. Maternal immunity in autism spectrum disorders: Questions of causality, validity, and specificity. *J. Clin. Med.* 9, 2590 (2020).

3. Anttila, V. *et al.* Analysis of shared heritability in common disorders of the brain. *Science (1979)*. 360, (2018).
4. Guerrera, S. *et al.* Autism Spectrum Disorder and Early Psychosis: a narrative review from a neurodevelopmental perspective. *Front. Psychiatry* 15, 1362511 (2024).
5. Davis, E. P. & Narayan, A. J. Pregnancy as a period of risk, adaptation, and resilience for mothers and infants. *Dev. Psychopathol.* 32, (2020).
6. Brown, A. S. Epidemiologic studies of exposure to prenatal infection and risk of schizophrenia and autism. *Dev. Neurobiol.* 72, (2012).
7. Atladóttir, H. Ó. *et al.* Maternal infection requiring hospitalization during pregnancy and autism spectrum disorders. *J. Autism Dev. Disord.* 40, (2010).
8. Kępińska, A. P. *et al.* Schizophrenia and influenza at the centenary of the 1918–1919 Spanish influenza pandemic: mechanisms of psychosis risk. *Front. Psychiatry* 11, 72 (2020).
9. Nestler, E. J. & Hyman, S. E. Animal models of neuropsychiatric disorders. *Nature Neuroscience 2010 13:10* 13, 1161–1169 (2010).
10. del Pino, I., Rico, B. & Marín, O. Neural circuit dysfunction in mouse models of neurodevelopmental disorders. *Curr. Opin. Neurobiol.* 48, 174–182 (2018).
11. Haddad, F. L., Patel, S. V. & Schmid, S. Maternal Immune Activation by Poly I:C as a preclinical Model for Neurodevelopmental Disorders: A focus on Autism and Schizophrenia. *Neurosci. Biobehav. Rev.* 113, 546–567 (2020).
12. Boulanger-Bertolus, J., Pancaro, C. & Mashour, G. A. Increasing role of maternal immune activation in neurodevelopmental disorders. *Front. Behav. Neurosci*. 12, (2018).
13. Smith, S. E. P., Li, J., Garbett, K., Mirnics, K. & Patterson, P. H. Maternal Immune Activation Alters Fetal Brain Development through Interleukin-6. *Journal of Neuroscience* 27, 10695–10702 (2007).
14. Antonson, A. M. *et al.* Moderately pathogenic maternal influenza A virus infection disrupts placental integrity but spares the fetal brain. *Brain Behav. Immun.* 96, (2021).
15. Liong, S. *et al.* Brain region-specific alterations in gene expression trajectories in the offspring born from influenza A virus infected mice. *Brain Behav. Immun.* 120, 488–498 (2024).
16. Crum, W. R. *et al.* Evolution of structural abnormalities in the rat brain following in utero exposure to maternal immune activation: A longitudinal in vivo MRI study. *Brain Behav. Immun.* 63, (2017).
17. Guma, E., Plitman, E. & Chakravarty, M. M. The role of maternal immune activation in altering the neurodevelopmental trajectories of offspring: A translational review of neuroimaging studies with implications for autism spectrum disorder and schizophrenia. *Neuroscience and Biobehavioral Reviews* vol. 104 Preprint at https://doi.org/10.1016/j.neubiorev.2019.06.020 (2019).
18. Velakoulis, D. *et al.* Hippocampal and amygdala volumes according to psychosis stage and diagnosis: A magnetic resonance imaging study of chronic schizophrenia, first-episode psychosis, and ultra–high-risk individuals. *Arch. Gen. Psychiatry* 63, 139–149 (2006).

19. Velakoulis, D. *et al.* Hippocampal volume in first-episode psychoses and chronic schizophrenia: A high-resolution magnetic resonance imaging study. *Arch. Gen. Psychiatry* 56, (1999).
20. Wannan, C. M. J. *et al.* Hippocampal subfields and visuospatial associative memory across stages of schizophrenia-spectrum disorder. *Psychol. Med.* 49, (2019).
21. Berk, M. *et al.* Pathways underlying neuroprogression in bipolar disorder: focus on inflammation, oxidative stress and neurotrophic factors. *Neurosci. Biobehav. Rev.* 35, 804–817 (2011).
22. Dutra, M. L. *et al.* Maternal immune activation induces autism-like behavior and reduces brain-derived neurotrophic factor levels in the hippocampus and offspring cortex of C57BL/6 mice. *Neurosci. Lett.* 793, 136974 (2023).
23. Griego, E., Segura-Villalobos, D., Lamas, M. & Galvan, E. J. Maternal immune activation increases excitability via downregulation of A-type potassium channels and reduces dendritic complexity of hippocampal neurons of the offspring. *Brain Behav. Immun.* 105, 67–81 (2022).
24. Mena, A. *et al.* Reduced prepulse inhibition as a biomarker of schizophrenia. *Front. Behav. Neurosci.* 10, (2016).
25. Choy, K. H. C. *et al.* Cognitive behavioral markers of neurodevelopmental trajectories in rodents. *Translational Psychiatry 2021 11:1* 11, 1–12 (2021).
26. Millar, J., Bilkey, D. K. & Ward, R. D. Maternal immune activation alters sensitivity to action-outcome contingency in adult rat offspring. *Brain Behav. Immun.* 63, (2017).
27. Liong, S. *et al.* Influenza A virus causes maternal and fetal pathology via innate and adaptive vascular inflammation in mice. *Proc. Natl. Acad. Sci. U. S. A.* 117, (2020).
28. Tustison, N. J. *et al.* N4ITK: Improved N3 bias correction. *IEEE Trans. Med. Imaging* 29, (2010).
29. Yu, Z. *et al.* A generalizable brain extraction net (BEN) for multimodal MRI data from rodents, nonhuman primates, and humans. *Elife* 11, e81217 (2022).
30. Modat, M. *et al.* Global image registration using a symmetric block-matching approach. *Journal of Medical Imaging* 1, (2014).
31. Modat, M. *et al.* Fast free-form deformation using graphics processing units. *Comput. Methods Programs Biomed*. 98, (2010).
32. Tole, S., Christian, C. & Grove, E. A. Early specification and autonomous development of cortical fields in the mouse hippocampus. *Development* 124, (1997).
33. Guma, E. *et al.* Early or Late Gestational Exposure to Maternal Immune Activation Alters Neurodevelopmental Trajectories in Mice: An Integrated Neuroimaging, Behavioral, and Transcriptional Study. *Biol. Psychiatry* 90, (2021).
34. Miller, J. G., Dennis, E. L., Heft-Neal, S., Jo, B. & Gotlib, I. H. Fine Particulate Air Pollution, Early Life Stress, and Their Interactive Effects on Adolescent Structural Brain Development: A Longitudinal Tensor-Based Morphometry Study. *Cerebral Cortex* 32, (2022).
35. Guma, E. & Chakravarty, M. M. Immune Alterations in the Intrauterine Environment Shape Offspring Brain Development in a Sex-Specific Manner. *Biological Psychiatry* vol. 97 12–27 Preprint at

https://doi.org/10.1016/j.biopsych.2024.04.012 (2025).

36. Estes, M. L. & McAllister, A. K. Maternal immune activation: Implications for neuropsychiatric disorders. *Science* vol. 353 Preprint at https://doi.org/10.1126/science.aag3194 (2016).
37. Bergdolt, L. & Dunaevsky, A. Brain changes in a maternal immune activation model of neurodevelopmental brain disorders. *Progress in Neurobiology* vol. 175 Preprint at https://doi.org/10.1016/j.pneurobio.2018.12.002 (2019).
38. Fair, D. A. *et al.* Functional brain networks develop from a 'local to distributed' organization. *PLoS Comput. Biol.* 5, (2009).
39. Fair, D. A. *et al.* The maturing architecture of the brain's default network. *Proc. Natl. Acad. Sci. U. S. A.* 105, (2008).
40. Zalesky, A. *et al.* Delayed development of brain connectivity in adolescents with schizophrenia and their unaffected siblings. *JAMA Psychiatry* 72, 900–908 (2015).
41. Kreitz, S. *et al.* Maternal immune activation during pregnancy impacts on brain structure and function in the adult offspring. *Brain Behav. Immun.* 83, (2020).
42. Mueller, F. S. *et al.* Behavioral, neuroanatomical, and molecular correlates of resilience and susceptibility to maternal immune activation. *Mol. Psychiatry* 26, (2021).
43. Harding, I. H. *et al.* Brain structure and degeneration staging in Friedreich ataxia: magnetic resonance imaging volumetrics from the ENIGMA-ataxia working group. *Ann. Neurol.* 90, 570–583 (2021).
44. DuPré, E. & Spreng, R. N. Structural Covariance Networks Across the Lifespan, From 6–94 Years of Age. https://doi.org/10.1101/090233 (2016) doi:10.1101/090233.
45. Aboud, K. S. *et al.* Structural Covariance Across the Lifespan: Brain Development and Aging Through the Lens of Inter-network Relationships. *Hum. Brain Mapp.* 40, 125–136 (2018).
46. Vijayakumar, N. *et al.* The Development of Structural Covariance Networks During the Transition From Childhood to Adolescence. *Sci. Rep.* 11, (2021).
47. Mitchell, E., Graham, A. L., Úbeda, F. & Wild, G. On maternity and the stronger immune response in women. *Nat. Commun.* 13, (2022).
48. Lins, B. R. *et al.* Prospective analysis of the effects of maternal immune activation on rat cytokines during pregnancy and behavior of the male offspring relevant to Schizophrenia. *eNeuro* 5, (2018).
49. Liu, Y. *et al.* Maternal immune activation induces sex-dependent behavioral differences in a rat model of schizophrenia. *Front. Psychiatry* 15, 1375999 (2024).
50. Kumari, V., Antonova, E. & Geyer, M. A. Prepulse inhibition and 'psychosis-proneness' in healthy individuals: An fMRI study. *European Psychiatry* 23, (2008).
51. Hammer, T. B. *et al.* Structural Brain Correlates of Sensorimotor Gating in Antipsychotic-Naive Men With First-Episode Schizophrenia. *Journal of Psychiatry and Neuroscience* 38, 34–42 (2013).
52. Gómez-Nieto, R., Hormigo, S. & López, D. E. Prepulse inhibition of the auditory startle reflex assessment as a hallmark of brainstem sensorimotor gating mechanisms. *Brain Sciences* vol. 10

Preprint at https://doi.org/10.3390/brainsci10090639 (2020).

53. Bezerra, T. O., Roque, A. C. & Salum, C. A Computational Model for the Simulation of Prepulse Inhibition and Its Modulation by Cortical and Subcortical Units. *Brain Sci.* 14, 502 (2024).
54. Suddath, R. L., Christison, G. W., Torrey, E. F., Casanova, M. F. & Weinberger, D. R. Anatomical abnormalities in the brains of monozygotic twins discordant for schizophrenia. *New England Journal of Medicine* 322, 789–794 (1990).
55. Adriano, F., Caltagirone, C. & Spalletta, G. Hippocampal volume reduction in first-episode and chronic schizophrenia: a review and meta-analysis. *The Neuroscientist* 18, 180–200 (2012).
56. Baglivo, V. *et al.* Hippocampal subfield volumes in patients with first-episode psychosis. *Schizophr. Bull.* 44, 552–559 (2018).
57. Schobel, S. A. *et al.* Differential targeting of the CA1 subfield of the hippocampal formation by schizophrenia and related psychotic disorders. *Arch. Gen. Psychiatry* 66, (2009).
58. Schobel, S. A. *et al.* Imaging Patients with Psychosis and a Mouse Model Establishes a Spreading Pattern of Hippocampal Dysfunction and Implicates Glutamate as a Driver. *Neuron* 78, 81–93 (2013).
59. Roeske, M. J., Konradi, C., Heckers, S. & Lewis, A. S. Hippocampal volume and hippocampal neuron density, number and size in schizophrenia: a systematic review and meta-analysis of postmortem studies. *Mol. Psychiatry* 26, (2021).
60. Fatemi, S. H. *et al.* The viral theory of schizophrenia revisited: abnormal placental gene expression and structural changes with lack of evidence for H1N1 viral presence in placentae of infected mice or brains of exposed offspring. *Neuropharmacology* 62, 1290–1298 (2012).

Figures

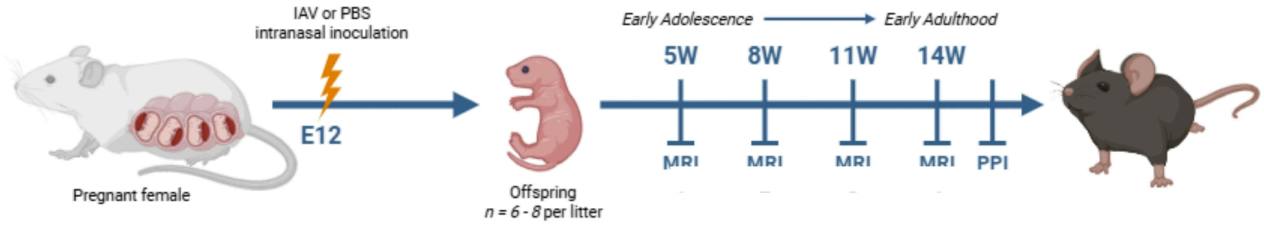


Figure 1

***Experimental design of the maternal influenza model and longitudinal offspring assessment*.** Pregnant C57BL/6J dams were intranasally inoculated at embryonic day 12 (E12) with either HKx31 influenza A virus (IAV; H3N2) or phosphate-buffered saline (PBS) control. Offspring underwent longitudinal in vivo

T2*-weighted MRI at 5, 8, 11 and 14 weeks of age, spanning early adolescence to early adulthood. Prepulse inhibition (PPI) testing was performed after the final MRI scan to assess sensorimotor gating, followed by euthanasia. Figure prepared with BioRender.

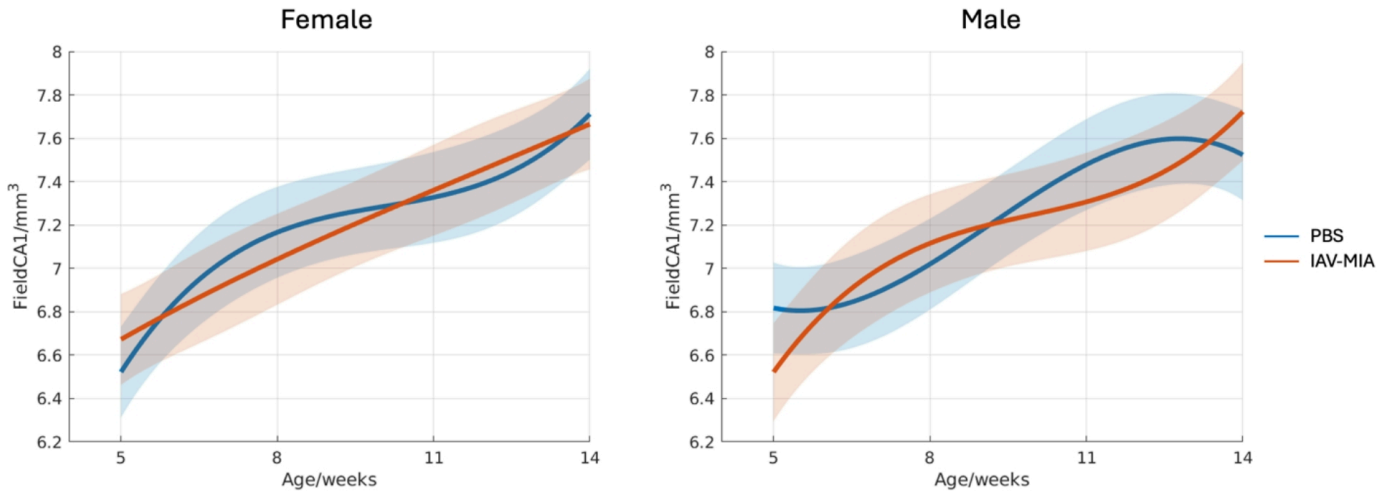


Figure 2

Maternal IAV exposure alters sex-specific developmental trajectories of hippocampal CA1 volume. Model-estimated longitudinal trajectories of CA1 volume are shown for male and female offspring in the IAV and PBS groups from 5 to 14 weeks of age. Blue lines represent the PBS group, and red lines represent the IAV group. Solid lines show marginal mean trajectories estimated from the linear mixed-effects model, and shaded bands indicate pointwise 95% confidence intervals for the estimated group mean. Following mixed-effects modelling and FDR correction, Field CA1 was the only atlas region showing significant treatment-related sex- and age-dependent developmental effects. The treatment × sex × age term was significant in CA1 (raw p = 0.000269; FDR-adjusted p = 0.0242; adjusted R^2 = 0.90).

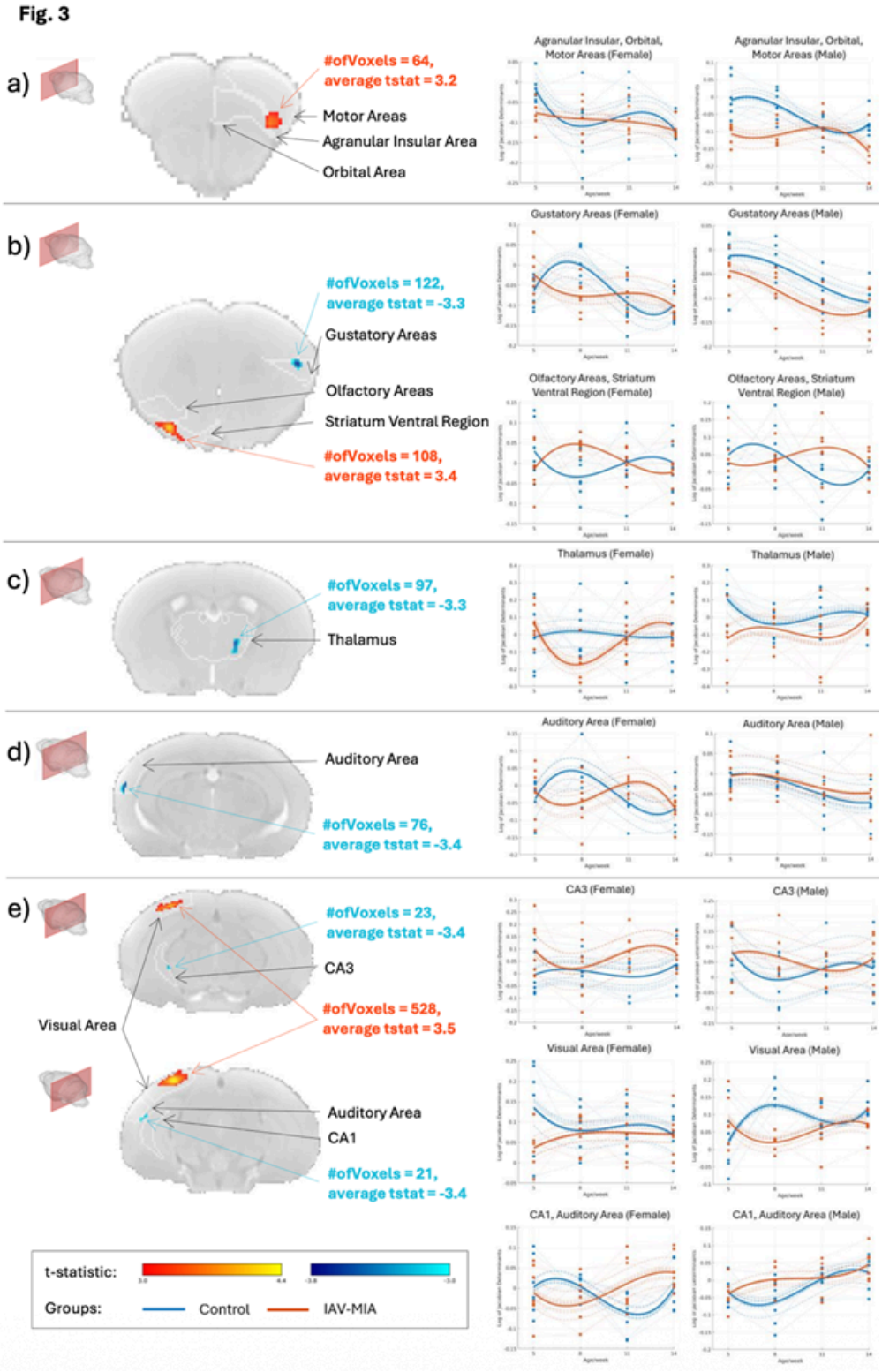


Figure 3

***Longitudinal tensor-based morphometry reveals sex-specific effects of maternal IAV exposure on local brain maturation. a-e shows different brain slices that have significant clusters*.** The left panel shows the t-statistic maps for the MIA × Age × Sex interaction effects from the mixed-effects model on longitudinal data. Significant areas are displayed with number of voxel count and averaged t-statistic. The right panels depict the longitudinal trajectories of significant clusters in various brain regions. Blue lines

represent the Control group, and red lines represent the MIA group. Connected dotted lines indicate data from the same animal, dashed lines represent model-predicted curves for each animal, and thick solid lines indicate the average of these model predictions. Dots represent individual animal data at each time point.

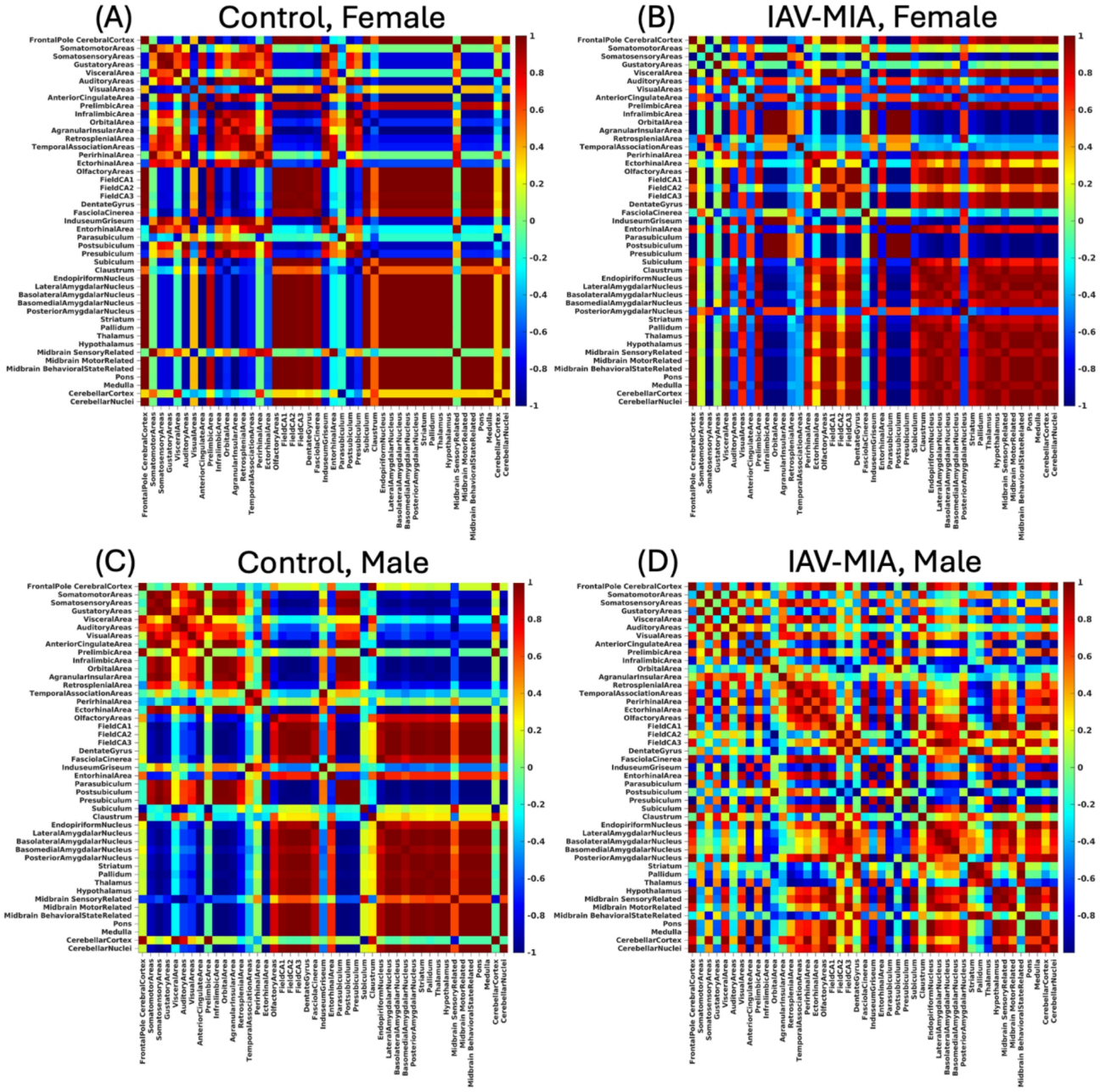


Figure 4

Maternal IAV exposure alters inter-regional structural correlation networks across adolescent brain development. Matrices derived from Spearman's rank correlation analysis between all possible pairs of brain regions. (A-D) are control, female; IAV-MIA, female; control, Male; IAV-MIA, Male. Eigenvalue spread

analysis, used here to quantify variability in correlation patterns, demonstrated marked differences in eigenvalue spreads across conditions: Female PBS (25.84), Female IAV (26.81), Male PBS (24.80), and Male IAV (17.63). Label-permutation testing (5,000 permutations) assessed the statistical significance of eigenvalue spread differences between treatment groups. The results indicated a significant difference for males (-7.168, $p < 0.0006$), suggesting that IAV altered inter-regional correlation variability, while a less significant difference was observed for females (+0.977, $p = 0.029$).

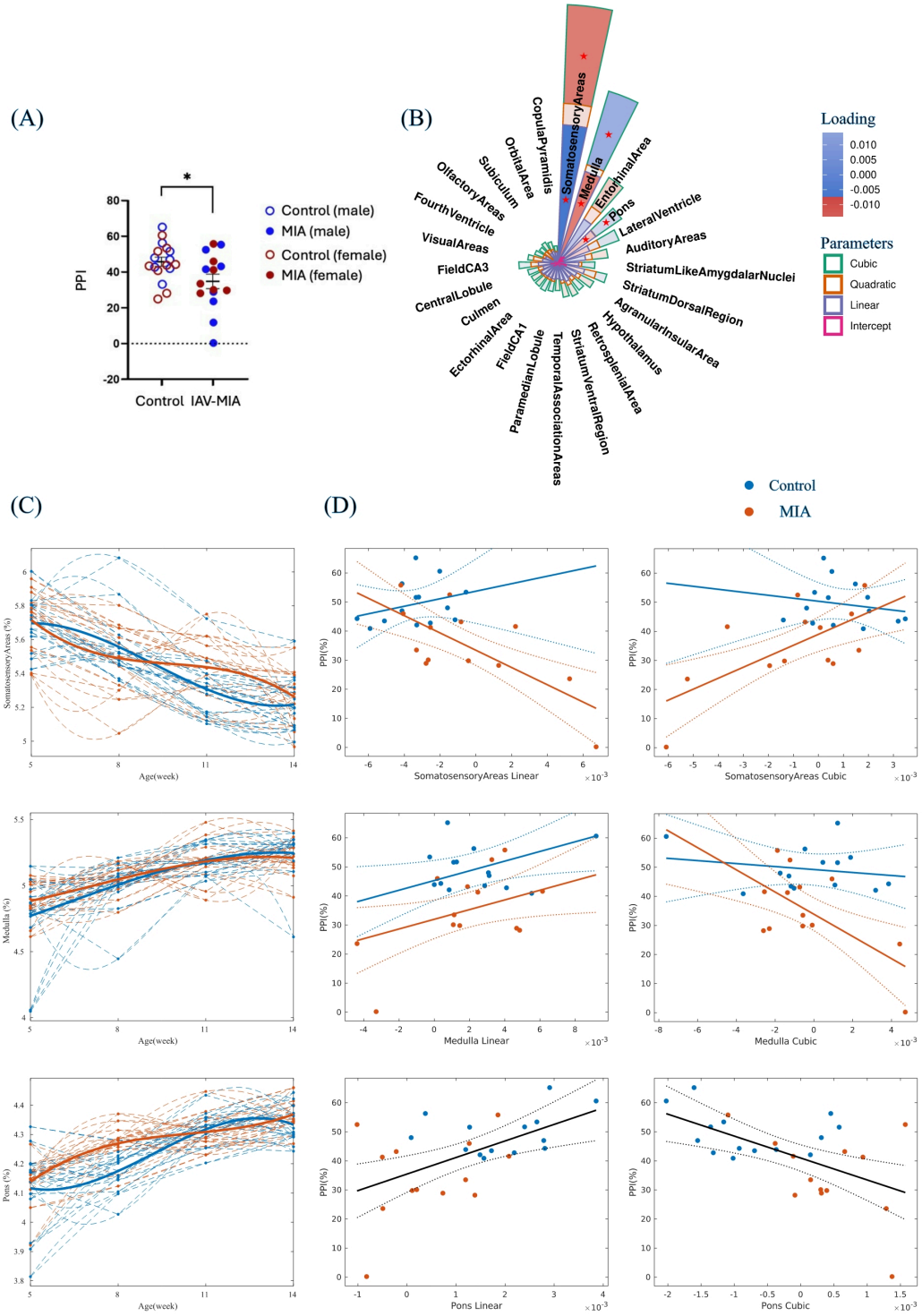


Figure 5

Maternal IAV exposure impairs sensorimotor gating and links altered brain maturation to behaviour.
(A) Prepulse inhibition (PPI) testing at 14.5 weeks showed reduced sensorimotor gating in offspring from IAV-infected dams compared with PBS controls (main effect of treatment: $F(1,27) = 5.261$, $p = 0.030$). No significant main effect of sex or treatment × sex interaction was detected.
(B) Partial least squares (PLS) regression identified a significant association between longitudinal brain developmental trajectory parameters and PPI performance. Radial plots show regional loadings for PLS Component 1, with trajectory terms represented from inner to outer rings: intercept, linear, quadratic and cubic. Colour indicates loading direction, and starred regions indicate significant bootstrap-supported contributors.
(C) Developmental trajectories for the dominant PLS-identified regions — somatosensory cortex, medulla and pons — across 5, 8, 11 and 14 weeks of age. Points represent individual observations and fitted curves show subject-level and/or group-level developmental trajectories for PBS and IAV-exposed offspring.
(D) Follow-up linear models show region- and trajectory-shape-specific relationships between brain maturation and PPI performance. MIA-related alterations in somatosensory, medullary and pontine developmental trajectories were significantly associated with impaired sensorimotor gating. Together, these analyses indicate that maternal IAV exposure produces behavioural deficits linked to altered maturation of cortical and brainstem circuits.

Supplementary Files

This is a list of supplementary files associated with this preprint. Click to download.

- DPengSupplement20260520.docx